

Electron Microscopy Analysis of Interfaces in Oxides for Energy Applications

Jonathan P. Winterstein, Chenchen Wang and C. Barry Carter

Chemical, Materials and Biomolecular Engineering Dept., University of Connecticut, 191 Auditorium Road Unit 3222, Storrs, CT 06269-3222

Oxide ceramics play an important role in many alternative energy technologies from catalysis [1] to solar energy [2] to solid-oxide fuel cells (SOFCs) [3]. In SOFCs the movement of ions and electrons across interfaces is a fundamental aspect of device operation and structure and chemistry at these interfaces is therefore crucial. Grain boundaries also play an important role in oxygen diffusion through SOFC electrolytes [4]. The presence of grain-boundary phases, in particular silicon oxide, is known to degrade electrochemical properties in ceria [5-7]. Aluminosilicate impurity phases have also been observed at the triple-phase boundary in SOFC anodes [8, 9]. Despite the critical role of interfaces, relatively few electron microscopy studies have been performed to investigate the nanoscale chemistry and structure of grain boundaries and phase boundaries in SOFC materials.

The interfaces investigated in this study include grain boundaries in ceria, grain boundaries in strontium-doped lanthanum manganite (LSM) and phase boundaries between ceria and LSM and between ceria and strontium-doped lanthanum ferrite (LSF). Particular attention was paid to the influence of impurities such as silica and alumina.

Powders of the starting materials were produced in house using solid-state reaction synthesis and wet-chemistry precipitation. In the case of ceria, high-purity powders from a commercial supplier were also investigated. TEM specimens were prepared by dimpling and ion milling discs of the pressed and sintered powders. TEM investigations were performed with a JEOL 2010 and a FEI T12.

Aluminum oxide impurities in the LSM powder segregated to the grain boundaries and triple junctions in the LSM polycrystal. During sintering the alumina reacted with the manganese to produce new grain boundary phases. Figure 1 contains bright-field TEM and dark-field STEM images of a triple junction between three LSM grains and STEM-XEDS maps showing the elemental segregation. Electron diffraction patterns of the manganese- and aluminum-containing product phase are consistent with the spinel-structured MnAl_2O_4 phase. XEDS line scans (not shown) indicate composition gradients within the LSM phase near the boundary with the grain-boundary phase. Powders produced using the wet-chemistry method avoid aluminum oxide impurities.

Cerium oxide grain boundaries were monitored before and after heat treatments. Grain-boundary grooving at the surface and the behavior of amorphous siliceous phases were analyzed. Figure 2 shows bright-field TEM images of an internal pore in the ceria polycrystal before and after heat treatment. Amorphous material is present at the grain-boundary-surface intersection but appears to move into the grain boundary after heat treatment. The shape of the grain-boundary groove changes in response to the heat treatment and surface faceting also evolves.

- [1] Z.-R. Tang *et al*, *J Catalysis* 249 (2007) 12.
 [2] J. E. Miller *et al*, *J Mater Sci* 43 (2008) 15.
 [3] B. C. H. Steele, *J Mater Sci* 36 (2001) 16.
 [4] A. Tschöpe, *J Electroceram* 14 (2005) 5.
 [5] T. S. Zhang, J. Ma, L. B. Kong and S. H. Chan, *J Mater Sci* 39 (2004) 6371.
 [6] R. Gerhardt, A. S. Nowick, M. E. Mochel and I. Dumler, *J Am Ceram Soc* 69 (1986) 647.
 [7] R. Gerhardt and A. S. Nowick, *J Am Ceram Soc* 69 (1986) 641.
 [8] A. Hauch, J. R. Bowen, L. T. Kuhn and M. Mogensen, *Electrochem Solid State Lett* 11 (2008) B38.
 [9] A. Hauch, S. H. Jensen, J. B. Bilde-Sorensen and M. Mogensen, *J Electrochem Soc* 154 (2007) A619.
 [10] JPW acknowledges support from the Air Force through an NDSEG Fellowship.

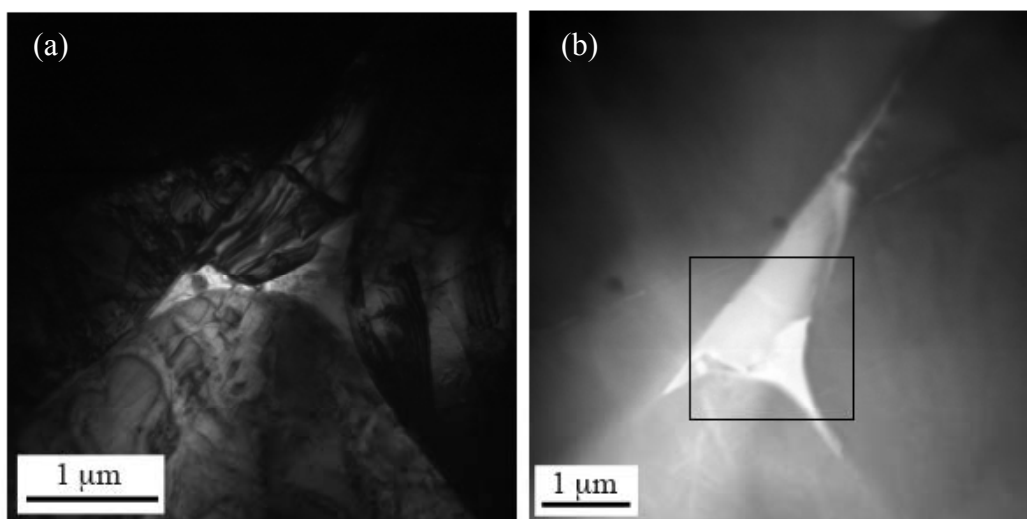


Figure 1: BF TEM (a) and DF STEM (b) image of a triple junction in an LSM polycrystal. STEM-XEDS maps (below) of the boxed region in (b) show the distribution of the cations present.

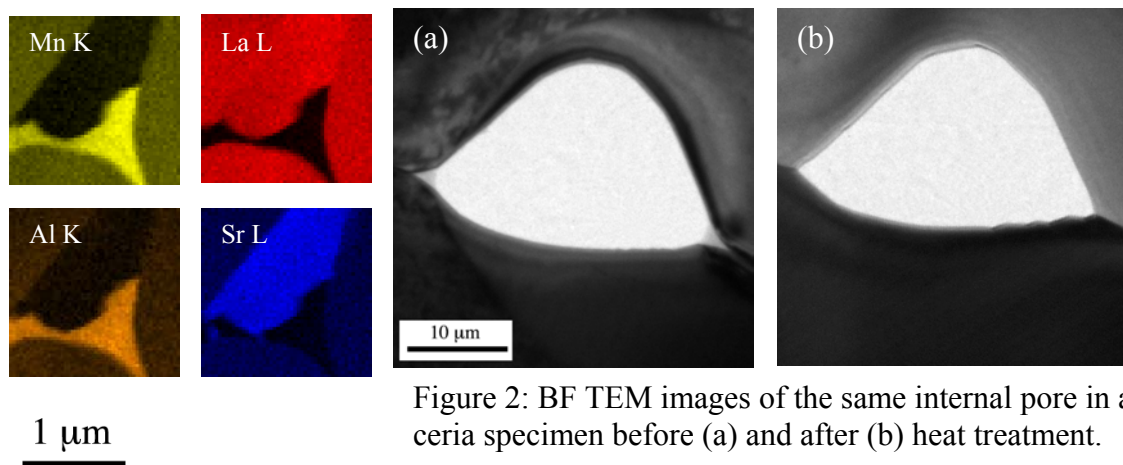


Figure 2: BF TEM images of the same internal pore in a ceria specimen before (a) and after (b) heat treatment.